

Theoretical study of Ga-based nanowires and the interaction of Ga with single-wall carbon nanotubes

E. Durgun, S. Dag, and S. Ciraci*

Department of Physics, Bilkent University, Ankara 06800, Turkey

(Received 26 April 2004; published 8 October 2004)

Gallium displays physical properties which can make it a potential element to produce metallic nanowires and high-conducting interconnects in nanoelectronics. Using first-principles pseudopotential plane method we showed that Ga can form stable metallic linear and zigzag monatomic chain structures. The interaction between individual Ga atom and single-wall carbon nanotube (SWNT) leads to a chemisorption bond involving charge transfer. Doping of SWNT with Ga atom gives rise to donor states. Owing to a significant interaction between individual Ga atom and SWNT, continuous Ga coverage of the tube can be achieved. Ga nanowires produced by the coating of carbon nanotube templates are found to be stable and high conducting.

DOI: 10.1103/PhysRevB.70.155305

PACS number(s): 73.22.-f, 68.43.Bc, 73.20.Hb, 68.43.Fg

I. INTRODUCTION

Nanowires display quantum properties which are of interest from fundamental, as well as technological point of view. Quantization of transversal electronic states and resulting quantum ballistic conductance and its stepwise variation in the course of stretching of wires have been studied extensively.^{1–10} The stepwise change of the cross section and “magic” atomic structures of a nanowire under tensile stress and the interplay between atomic structure and quantized conductance have been of particular interest in recent years.^{4,6,11–19}

From the technological point of view, fabrication of stable metallic wires having diameter in the range of nanometer has been crucial for the realization of high-conducting, low-energy dissipating²⁰ interconnects in nanoelectronics.²¹ Recent experimental^{22,23} and theoretical studies^{24,25} have demonstrated that such nanowires can be produced in a reproducible manner by depositing atoms on a single-wall carbon nanotube (SWNT). Continuous Ti coating of varying thicknesses and quasicontinuous coatings of Ni and Pt were obtained by using electron-beam evaporation techniques.^{22,23} Not only metallic connects but also the contacts of metal electrodes themselves are crucial for the operation of devices based on nanotubes.²⁶ Low resistance Ohmic contacts to metallic and semiconducting SWNT's were achieved by Ti and Ni atoms.²⁶ The formation of Schottky barrier at the contact between metal and SWNT has been found to be responsible for the operation of field emission transistors made from SWNT's.²⁷

The electronic and magnetic properties of carbon nanotubes (CNT) can be functionalized by adsorbing different metal atoms.^{28,29} It has been shown that transition-metal atom adsorbed SWNT's have magnetic ground states with significant magnetic moment.²⁹ The possibility of filling open nanotubes with liquid by capillary suction is predicted³⁰ and filling of the tube with molten lead through capillary action is achieved.³¹ Moreover, temperature measurement by means of a Ga-filled CNT thermometer with diameter smaller than 150 nm is reported.³² Liquid Ga has also potential application as microswitches/nanoswitches.

Gallium has attracted our interest due to its unusual physical properties. It is the only metal, except for mercury, cesium, and rubidium, which can be liquid near room temperatures; this makes its use possible in high-temperature thermometers. It has one of the longest liquid ranges of any metal and has a low vapor pressure even at high temperatures. Ga is stable in air and water and high-purity gallium is attacked only slowly by mineral acids. Because of these properties Ga can make interesting wire structures. Consequently, Ga adsorption or Ga coating of SWNT can be of particular interest from the electronic devices point of view.

In this paper we present a systematic study on Ga based nanowires. In the first part, binding geometry, cohesive energy, electronic properties, and stability of various Ga monatomic chain structures are analyzed. In the second part, single Ga adsorption on various sites of the zigzag (8,0) SWNT is studied. Our prime objective is to reveal the character and geometry of the bonding and to understand the effect of the adsorption on physical properties of SWNT. In this context we also examined the formation of a Ga monatomic chain on the (8,0) tube. Finally in the third part, we considered the possibility of producing conducting wires through Ga coating of SWNT templates and hence investigated the properties of the Ga covered (8,0) tubes. We found that Ga monatomic chains are metallic and stable even at 800 K. Single Ga atom can be adsorbed to SWNT both from outside and inside with a significant binding energy. We showed that Ga atoms may form continuous and stable coverage of SWNT that transforms the semiconducting tube into a high-conducting metal. Our results suggest that Ga is an element which can functionalize SWNT to make interconnects or contacts for device applications.

II. METHOD OF CALCULATIONS

First-principles total energy and electronic structure calculations have been performed using the pseudopotential plane-wave method³³ within the generalized gradient approximation.³⁴ Various structures are treated with a periodically repeating tetragonal supercell method. Brillouin-

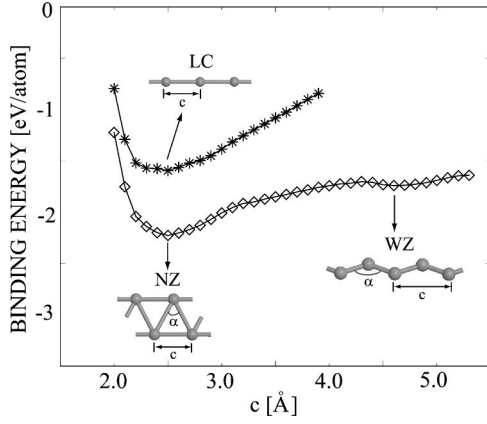


FIG. 1. Variation of binding energy E_b of monatomic chain structures as a function of lattice parameter c . Various chain structures, linear chain (LC), planar wide angle zigzag (WZ), and narrow angle zigzag (NZ) structures are described by insets.

zone integrations are performed with 11 special \mathbf{k} points within Monkhorst-Pack special \mathbf{k} -point scheme.³⁵ All atomic positions in the supercell as well as the supercell lattice parameter c are fully relaxed using the conjugate gradient method. The analysis of the stability at finite temperature has been carried out by relaxing the optimized structures at 800–1000 K using *ab initio* molecular-dynamics (MD) method with Nosé thermostat.

The binding energy (or cohesive energy) E_b for the chain structures is calculated by

$$E_b = E_T[\text{Ga}] - E_T[\text{Ga-Chain}] \quad (1)$$

in terms of the total energy of single, free Ga atom, $E_T[\text{Ga}]$, and the total energy of chain structure per atom, $E_T[\text{Ga-Chain}]$, which have been calculated in the same supercell. In the study of Ga covered SWNT, the average binding energy of Ga atom adsorbed on a SWNT is calculated by

$$\overline{E_b} = \{E_T[\text{Ga}] + E_T[\text{SWNT}] - E_T[\text{SWNT} + N\text{Ga}]\}/N, \quad (2)$$

where $E_T[\text{SWNT}]$ is the total energy (per cell) of fully relaxed bare SWNT and $E_T[\text{SWNT} + N\text{Ga}]$ is the total energy (per cell) of the SWNT covered by N Ga atoms. In these calculations $E_b > 0$ indicates stable binding. We considered the zigzag (8,0) tube as a prototype SWNT in our study. The lattice parameter of the bare, relaxed (8,0) tube is specified as $c_{\text{SWNT}} = 4.2 \text{ \AA}$, and the cohesive energy is calculated to be $E_b = 9.1 \text{ eV}$ per carbon atom.

III. Ga MONATOMIC CHAIN STRUCTURES

Earlier studies showed that atoms of some elements can form stable monatomic chain structures.^{12–14,18,19,36–39} For example, it has been found that Au and Al can form three different chain structures,^{36,39} namely, the linear chain (LC), planar wide angle (WZ), and narrow angle (NZ) zigzag structures described in insets of Fig. 1. While LC has lowest, NZ has the highest cohesive energy per atom. Similar trends have been found also for Group IV elements, such as Si, Ge,⁴⁰ but not C. Interestingly, C atom forms only stable LC

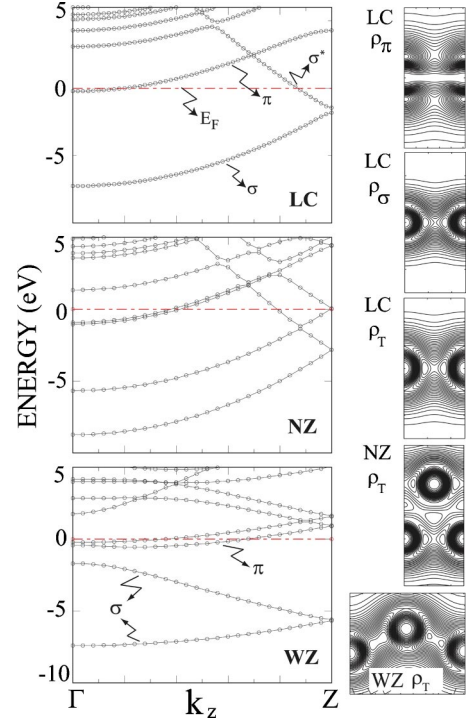


FIG. 2. Left panels: Calculated energy-band structures of Ga LC, NZ, and WZ monatomic chain structures. Zero of the energy is set at the Fermi level and shown by dash-dotted line. Right panels: Counter plots of the band charge density (ρ_σ, ρ_π) of LC structure and total charge density (ρ_T) of all three chain structures on a plane passing through the Ga-Ga bonds.

structure, and WZ and NZ structures are unstable and change into LC. Usually the cohesive energies of LC and WZ are very close. Here we analyzed LC, WZ, and NZ chain structures of Ga atom. Our results are summarized in Fig. 1. The binding energy versus lattice parameter, c curves, i.e., $E_b(c)$ per atom, agrees well with previous first-principles studies for Au, Al wires and AuZn, AuMg alloys.^{36,38,39,41} We found among three optimized chain structures NZ structure with $c = 2.6 \text{ \AA}$ and $\alpha \approx 55^\circ$ has the highest binding energy ($E_b = 2.2 \text{ eV}$), and WZ appears a weak minimum at $c = 4.6 \text{ \AA}$ corresponding to $\alpha \approx 131^\circ$ with an intermediate binding energy ($E_b = 1.8 \text{ eV}$). LC structure has the lowest binding energy ($E_b = 1.6 \text{ eV}$) with optimized $c = 2.6 \text{ \AA}$ and $\alpha = 0$.

The stability of these chain structures has been tested by raising the temperature to 800 K. To this end we carried out *ab initio* MD calculations for 250 time steps using a relatively larger supercell containing four unit cells. We found that LC maintained its string shape, but its strict linearity has been destroyed due to the displacements of atoms at finite temperature. Overall structure of NZ also has been maintained, but WZ has been excited at high temperature and eventually trapped at the minimum of LC structure.

Analysis of the electronic band structure shows that all three chain structures studied here are metallic. The calculated energy-band structures are illustrated in the Fig. 2 for each geometry. The lowest band of LC is due to the σ bond and is derived 4s and 4p_z valence orbitals of Ga. The doubly

degenerate π band is formed from the bonding combination of $4p_x(4p_y)$ orbitals which are perpendicular to the axis of LC. Small displacement of every second Ga atom perpendicular to the axis of the WZ is a distortion that doubles the unit cell but lowers the binding energy. The bands of WZ structure can be derived from those of LC in Fig. 2; by going from LC to WZ all bands of LC are folded and due to the breaking of cylindrical symmetry the doubly degenerate π and π^* bands are split. Also the σ^* band of LC which dips into the Fermi level near Z is lifted and becomes unoccupied in WZ. The bands of NZ structure are rather different from those of LC and WZ structures, since each atom of NZ has four nearest neighbors. The character of the bonds is illustrated by the charge density contour plots in Fig. 2. Except delocalization due to σ^* -band dipping into the Fermi level, the charge density $\rho_T(\mathbf{r})$ of LC structure depicts a double-bond character. The double-bond character is strengthened in the WZ structure because of the lifting of the σ^* band from the Fermi level. The total charge density of the NZ structure becomes more uniform and metal-like in the plane of Ga atoms.

The electrical current through a metallic infinite nanowire with infinite mean free path $l_m \rightarrow \infty$ is given by Landauer-type expression⁴² $I = \sum_i 2\eta_i e v_i [D(E_F + eV_b) - D_i(E_F)]$ in terms of degeneracy η_i , group velocity v_i , and density of states of each subband i crossing the Fermi level.¹⁰ Then the ballistic conductance becomes $G = \sum_i \eta_i 2e^2/\hbar$, namely, the number of bands crossing the Fermi level times $G_0 (= 2e^2/h)$. Based on the band structures presented in Fig. 2, the ballistic conductances of infinite Ga chain structures are found to be $3G_0$, $5G_0$ and $2G_0$ for LC, NZ, and WZ structures, respectively. Owing to the small displacement of every second atom in WZ structure one channel of LC is closed. In spite of two strands in NZ its conductance is smaller than the conductance of two parallel LC.

IV. Ga ATOM ADSORPTION ON (8,0) SWNT

Earlier it has been shown that the electronic properties of a SWNT can be dramatically modified by the adsorption of foreign atoms.^{29,43} For the adsorption on SWNT, we considered four possible sites as an initial position of Ga before structure optimization, namely, *H* site above (outside—exo) or below (inside—endo) the surface hexagon, the *Z* and *B* sites above the zigzag and axial C-C bonds, and the *T* site above carbon atoms. The lowest energy binding site is determined by minimizing the total energy of SWNT having a Ga atom adsorbed at one of those sites described in Fig. 3. To eliminate the Ga-Ga interaction, we considered a single Ga atom adsorbed in every two unit cells of SWNT. Accordingly the lattice parameter of the supercell is approximately twice the lattice parameter of SWNT, i.e., $c \sim 2c_{SWNT}$. To find the lowest binding energy for a given adsorption site all atomic positions (SWNT+Ga) and the supercell lattice parameter have been relaxed. The long-range van der Waals interaction, E_{vdw} , is expected to be much smaller than the chemisorption binding energy and is omitted in the present calculations. The calculated E_b 's for both SWNT and graphene are listed in Table I. The *H* site is found to be energetically most fa-

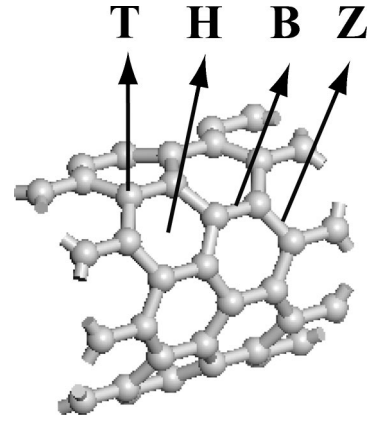


FIG. 3. A schematic description of different binding sites of individual atoms adsorbed on a zigzag (8,0) tube. *H*, hollow; *B*, bridge; *Z*, zigzag; *T*, top site.

vorable site among external sites. However, the binding of Ga adsorbed at the *H* site, but inside the tube, yields $E_b = 2.9$ eV, which is stronger than corresponding external adsorption. The binding of Ga adsorbed inside is stronger, since the adsorbate interacts with more C atoms as compared with Ga adsorbed outside. According to the Mulliken analysis 2.1 electrons are transferred from inside Ga to SWNT, while only 1.1 electrons are transferred to SWNT when Ga is adsorbed outside. These values are consistent with E_b 's calculated for inside (endo) and outside (exo) adsorptions. The binding energy is reduced to 1.1 eV for Ga adsorbed on the graphene. This is an expected result and can be explained by the curvature effect which is the primary factor that strengthens the bonding on the SWNT.^{44–46}

The electronic structure analysis indicates that Ga adsorption both inside and outside (in fact, forming a Ga LC attached to SWNT with $c \sim 2c_{SWNT}$) metallizes the semiconducting SWNT. The calculated energy-band structures and local density of states (LDOS) for both Ga and SWNT are presented in Fig. 4. According to LDOS analysis, the band which crosses E_F is derived mainly from SWNT conduction band. This result combined with the Mulliken analysis, yielding a charge transfer of 1.1 (2.1) electrons from exo (endo) adsorbed Ga to SWNT, suggests that Ga electrons are donated to the lowest conduction bands of the bare (8,0) tube. As a result, initially empty conduction band of SWNT is gradually populated and also modified upon adsorption of Ga, which makes periodic Ga+SWNT system (as treated within supercell geometry) a metal. Present results are consistent with the previous Al+SWNT studies.²⁹ These results obtained from the supercell structure, where Ga atom adsorbed on the SWNT is repeated periodically, suggest that the doping of a SWNT by an individual Ga atom results in a

TABLE I. Binding energy E_b and average Ga-C distance of Ga adsorbed at different sites on the (8,0) tube.

	<i>H</i> (exo)	<i>H</i> (endo)	<i>B</i>	<i>T</i>	<i>Z</i>	Graphene <i>H</i>
E_b (eV)	1.7	2.9	1.4	1.4	1.4	1.1
d (Å)	2.4	2.7	2.4	2.3	2.4	2.9

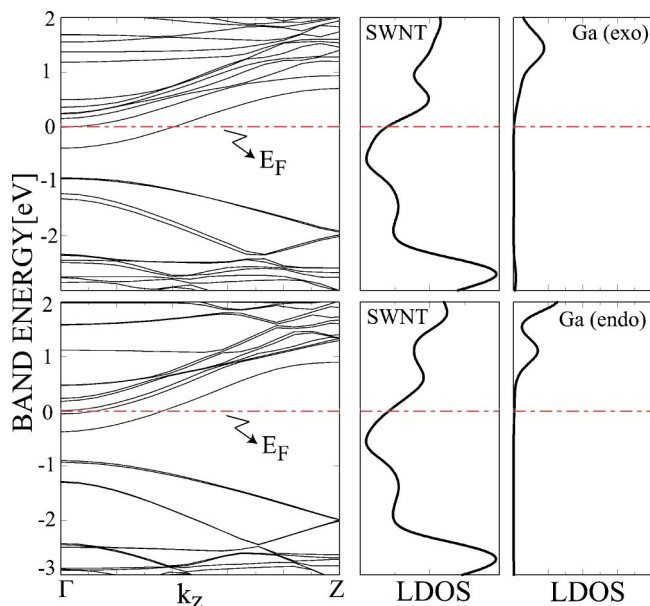


FIG. 4. Energy-band structures are calculated for Ga adsorbed at the H site of the $(8,0)$ tube with periodicity $c \sim 2c_{SWNT}$ and local density of states, LDOS, calculated at SWNT and at the adsorbed Ga atom. Upper panels are for exo adsorption of Ga; lower ones are for endo adsorption. Zero of the energy is set at the Fermi level and is shown by dash-dotted lines.

donor state. The charge density contour plots calculated on a plane passing through exo (endo) adsorbed Ga atom are presented in Fig. 5. The distribution of charge density between Ga and SWNT is consistent with the above arguments related with the bonding of Ga atom.

V. Ga ZIGZAG CHAIN ON SWNT

The discussion in the preceding section shows that the semiconducting SWNT is metallized as a result of Ga ad-

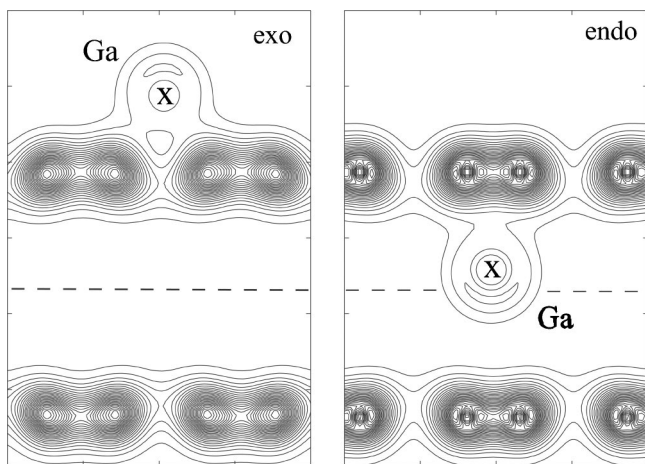


FIG. 5. Counter plots of the total charge density $\rho_T(\mathbf{r})$ of exo adsorbed Ga and endo adsorbed Ga on the H site of the SWNT surface. The chemical bonding and charge transfer from Ga to SWNT are revealed from counter plots. The axis of the SWNT is shown by dashed lines.

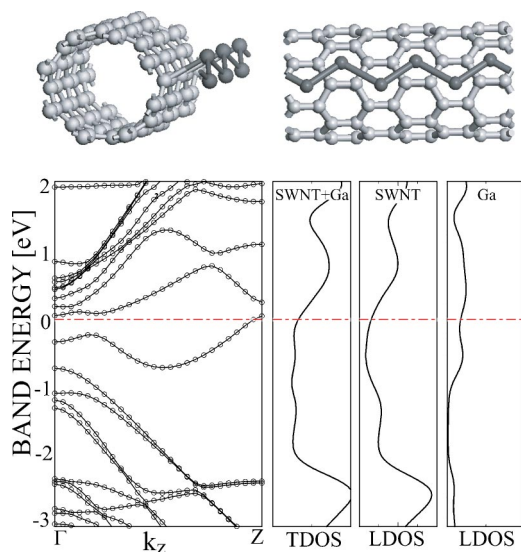


FIG. 6. Calculated energy band structure, total density of states (TDOS), and local density of states (LDOS) at the SWNT and at the Ga atoms of the Ga-zigzag chain adsorbed on the $(8,0)$ tube. Zero of the energy is set at the Fermi level and is shown by dash-dotted line. The adsorption geometry is described by inset, where dark and light balls indicate Ga and C atoms, respectively.

sorption, forming a chain with the lattice parameter $2c_{SWNT}$ within the supercell geometry. Now we explore the effect of the chain formation of adsorbates and investigate the Ga zigzag chain on SWNT. The initial structure is obtained by placing a Ga atom at the adjacent H site along the axis the tube. The structure of relaxed Ga zigzag chain on SWNT is shown in Fig. 6. Here the Ga-Ga nearest-neighbor distance of 2.6 \AA is close to what is obtained in free WZ structure. However, in the present case Ga-SWNT distance is increased from 2.4 \AA (the value corresponding to a single exo Ga atom adsorption) to $2.9\text{--}3.5 \text{ \AA}$. The strong Ga-Ga coupling in the adsorbed zigzag chain reduces the charge transfer from Ga atom to the SWNT. This way, while Ga-SWNT bond is weakened, the Ga-Ga double bond is formed. This situation is consistent with the calculated binding energy and charge transfer. Mulliken analysis yields 0.4 electrons transferred from each Ga atom of the adsorbed WZ chain to SWNT. This value is 0.7 electrons smaller than that transferred in single Ga adsorption. As for the binding energy between zigzag chain and SWNT is calculated to be 0.4 eV .

The strong bonding between Ga-Ga, but weak bonding between Ga-SWNT, is reflected to the calculated band structure shown in Fig. 6. Two bands around E_F , one almost fully occupied and the other almost empty, are reminiscent of the π bands of the free WZ in Fig. 2. The weak Ga-SWNT interaction causes distortion of these π bands. Calculated LDOS's are in compliance with the present explanation.

VI. Ga COVERAGE OF SWNT

Following the adsorption of Ga atom ($c=2c_{SWNT}$) and Ga-zigzag chain ($c=c_{SWNT}$) we next study the Ga coverage of SWNT. To this end we attach one Ga atom to each H site

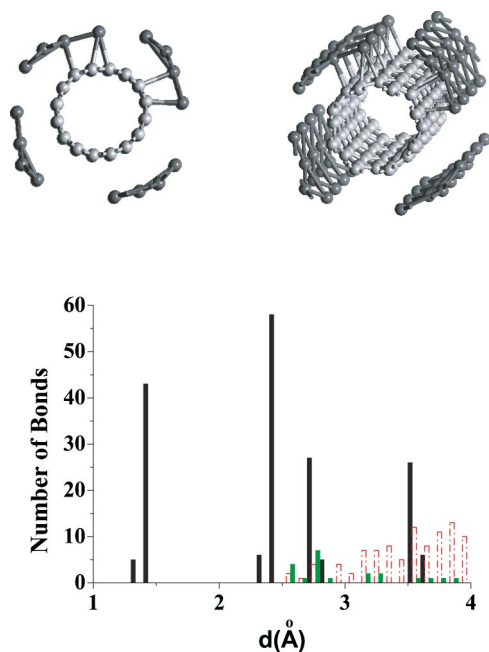


FIG. 7. Intermediate coating obtained by 16 Ga atoms located above each hexagon on the surface of SWNT. Distribution of Ga-Ga, Ga-C, and C-C distances are illustrated by gray, dotted, and dark histograms, respectively, in the plot. Ga stripes and SWNT template are shown by dark and light balls.

on the SWNT, namely, 16 Ga atoms per unit cell. Upon relaxation of the structure Ga atoms move from their original position so that their distance from the surface of the SWNT increases. Owing to the relatively strong Ga-Ga interaction, Ga-Ga distance is reduced while Ga-SWNT distance is increased. At the end, Ga islands or stripes are formed above the SWNT as shown in Fig. 7. In the same figure the distribution of Ga-Ga, Ga-C, and C-C interatomic distances are presented by histograms. We note that there are two different C-C bond distances in the SWNT template. Each of these islands or stripes forms a metallic domain on the surface of SWNT. In order to obtain a more uniform coverage we first add four more Ga atoms between four islands seen in Fig. 7. Upon relaxation Ga atoms rearrange and start to form zigzag chain structures on the surface of SWNT.

Finally, two more Ga atoms are added to fill vacant sites of Ga coating. Further optimization of the structure has led to a continuous coverage with stable zigzag Ga structures on SWNT as illustrated in Fig. 8. The distribution of interatomic distances is also presented in the same figure. In the final structure Ga nearest-neighbor distances range between 2.5 and 3.0 Å and Ga-C distance ranges between 2.4 and 4.0 Å. The circular cross section of SWNT becomes slightly elliptic. Owing to the weak interaction between SWNT and Ga, the length of the C-C bond and the second nearest-neighbor distances do not display significant changes and variations as compared to the bare SWNT. However, the elliptic deformation of SWNT gives rise to the dispersions in the third and fourth nearest-neighbor distances. Nonuniformities of the Ga coating are attributed to the lattice mismatch between SWNT and Ga two-dimensional (2D) lattice. The charge transfer is about 0.4 electrons per Ga atom and like the intermedi-

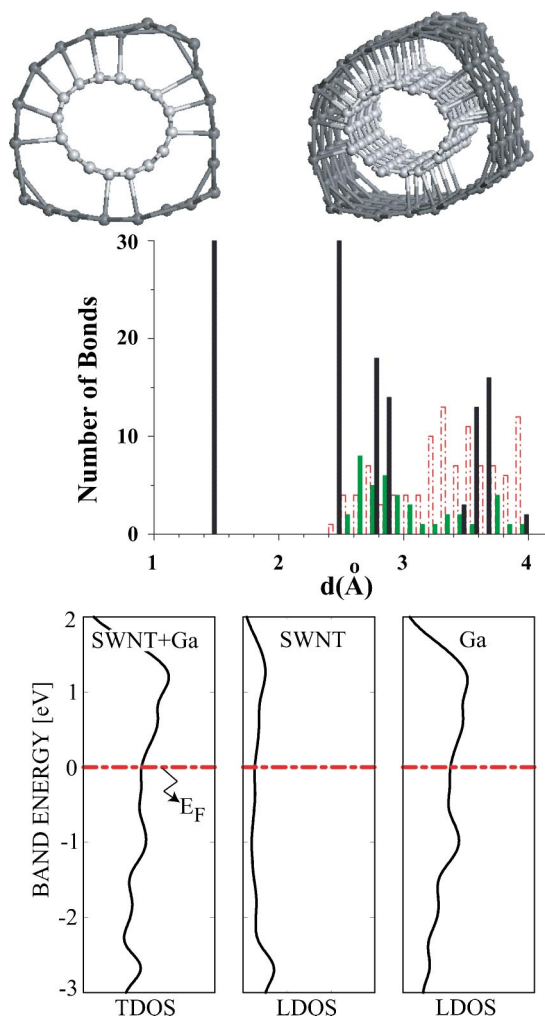


FIG. 8. Top and side views of fully Ga covered (8,0) SWNT. The supercell incorporates 32 C [one unitcell of (8,0) SWNT] and 22 Ga atoms. Distributions of first and second nearest-neighbor Ga-Ga, Ga-C, and C-C distances are presented by gray, dotted, and dark histograms, respectively. Total density of states (TDOS) and local density of states (LDOS) calculated at the SWNT and at the Ga coating are shown in the lower panels.

ate coverage, the system is metallic. It is expected that upon the formation of thick Ga coating involving several Ga layers around SWNT the charge transfer further decreases and Ga-C distance increases. Under these circumstances a potential barrier can develop between the metallic Ga coating and semiconducting SWNT. Such a situation can be exploited as metal-semiconductor junction device.

The electronic structure having several bands crossing the Fermi level indicates that Ga coated SWNT is high conducting. The origin of the metallicity of Ga covered SWNT, which was a semiconductor in the absence of Ga atoms, is determined by total density of states and LDOS indicating that the high state density originates from the Ga atoms. The nonuniformity of the interatomic distances which may destroy the one-dimensional periodicity can give rise to the localization of current transporting states.⁴⁷ This is characterized by the localization length ξ . Owing to the tubular nature and infinite cross section we expect that for Ga-covered

SWNT $\xi \sim l_m(D/\lambda_F)^\alpha$ with $1 < \alpha < 2$. Here D is the diameter of the wire and λ_F is the Fermi wavelength. Our estimation suggests that ξ is in fact much larger than typical length scale of interconnects.

The stability of Ga coating is important to produce a stable conducting nanowire. The *ab initio* MD calculation of fully Ga covered SWNT at 1200 K has shown that the system was stable after 50 time steps. Continuity was maintained; neither clusterings nor vacancies have occurred. Furthermore, we tested the stability of Ga coating (tubular structure) by deleting SWNT and by relaxing it at $T=0$. After full relaxation tubular form has remained. It appears that Ga tube made of zigzag chains contributes to the stability of Ga covered SWNT. The wetting of liquid metals on solid metals and nonmetallic materials had been studied extensively to form composites with exceptional properties.⁴⁸ We believe that present results are relevant to the wettability of graphite and SWNT by liquid Ga to produce Ga-matrix composites or to form Ga intermediates to attach other metals.

VII. CONCLUSION

The present study has revealed interesting features of Ga element in forming chain structure and also in coating of a semiconducting SWNT. Ga forms monatomic linear and zigzag chain structures which are metallic and stable even at high temperatures. The zigzag structures are energetically more favorable than the linear structure.

The electronic properties of SWNT can be modified via single Ga adsorption. Individual Ga adsorbed inside or outside the tube gives rise to donor states. This, in turn, makes the initially semiconducting SWNT metallic at finite tem-

perature due to charge transfer from Ga atoms to nanotube. SWNT can serve as a template for constructing stable Ga chains on its surface. The $4p$ electrons from Ga chain are partially transferred to SWNT and generate additional states around E_F . The band-structure analysis shows that initially semiconducting SWNT transforms into a metal with adsorption of Ga atoms.

Finally, it is shown that the formation of continuous Ga coverage of SWNT can be achieved. This possibility revealed by a theoretical study requires, of course, the elaboration of growth conditions which determines the quality of growth. The circular cross section changes into elliptical form after the full coverage of Ga. The SWNT becomes a quasi-1D metal with high state density at E_F . As $3d$ orbitals of Ga behave like semicore states, the ground state of Ga covered SWNT system is nonmagnetic. The *ab initio* MD calculations at 1200 K have shown that Ga coating is stable even at high temperatures. These results suggest that a SWNT can be used as template to produce high-conducting nanowires by using Ga coverage. Ga atoms being liquid at room temperature and stable in air water can be used to produce 1D conductors, thin metallic connects, and nanometersized electronic devices which may find technological applications in nanoscience. In particular, the conductivity of liquid Ga-filled SWNT can be exploited as nanoswitch.

ACKNOWLEDGMENTS

This work was partially supported by the National Science Foundation under Grant No. INT01-15021 and TÜBİTAK under Grant No. TBAG-U/13(101T010). Part of computations have been carried out at ULAK-BIM computer center. S.C. acknowledges partial financial support from Academy of Science of Turkey.

*Electronic address: ciraci@fen.bilkent.edu.tr

¹J. K. Gimzewski and R. Möller, Phys. Rev. B **36**, 1284 (1987).
²N. D. Lang, Phys. Rev. B **36**, 8173 (1987).
³J. Ferrer, A. M. Rodero, and F. Flores, Phys. Rev. B **38**, 10 113 (1988).
⁴S. Ciraci and E. Tekman, Phys. Rev. B **40**, 11 969 (1989); E. Tekman and S. Ciraci, Phys. Rev. B **43**, 7145 (1991).
⁵T. N. Todorov and A. P. Sutton, Phys. Rev. Lett. **70**, 2138 (1993).
⁶N. Agraït, J. G. Rodrigo, and S. Vieira, Phys. Rev. B **47**, 12 345 (1993); N. Agraït, G. Rubio, and S. Vieira, Phys. Rev. Lett. **74**, 3995 (1995).
⁷J. I. Pascual, J. Méndez, J. Gómez-Herrero, A. M. Baró, N. Garcia, and V. T. Binh, Phys. Rev. Lett. **71**, 1852 (1993).
⁸L. Olesen, E. Laegsgaard, I. Stensgaard, F. Besenbacher, J. Schiøtz, P. Stoltze, K. W. Jacobsen, and J. K. Nørskov, Phys. Rev. Lett. **72**, 2251 (1994).
⁹J. M. Krans, C. J. Muller, I. K. Yanson, Th. C. M. Govaert, R. Hesper, and J. M. van Ruitenbeek, Phys. Rev. B **48**, 14 721 (1994).
¹⁰For the review of the subject see S. Ciraci, A. Buldum, and I. P. Batra, J. Phys.: Condens. Matter **13**, R537 (2001).
¹¹J. I. Pascual, J. Mendez, J. Gomez-Herrero, A. M. Baro, N. Garcia, U. Landman, W. D. Luedke, E. N. Bogachek, and H. P.

Cheng, Science **71**, 1793 (1995).
¹²H. Mehrez and S. Ciraci, Phys. Rev. B **56**, 12 632 (1997).
¹³O. Gülseren, F. Ercolessi, and E. Tosatti, Phys. Rev. Lett. **80**, 3775 (1998).
¹⁴M. R. Sørensen, M. Brandbyge, and K. W. Jacobsen, Phys. Rev. B **57**, 3283 (1998).
¹⁵E. Tosatti, S. Prestipino, S. Kostlmeier, A. Dal Corso, F. D. Di Tolla, Science **291**, 288 (2001).
¹⁶Y. Kondo and K. Takayanagi, Science **289**, 606 (2000); **395**, 780 (1998).
¹⁷Y. Oshima, H. Koizumi, K. Mouri, H. Hirayama, K. Takayanagi, and Y. Kondo, Phys. Rev. B **65**, 121401 (2002).
¹⁸H. Ohnishi, Y. Kondo, and K. Takayanagi, Nature (London) **395**, 780 (1998).
¹⁹A. I. Yanson, G. R. Bollinger, H. E. Brom, N. Agraït, and J. M. Ruitenbeek, Nature (London) **395**, 783 (1998).
²⁰Z. Yao, C. L. Kane, and C. Dekker, Phys. Rev. Lett. **84**, 2941 (2000).
²¹A. Aviram and M. Ratner, Chem. Phys. Lett. **29**, 277 (1974).
²²H. Dai, E. W. Wong, Y. Z. Lu, S. Fan, and C. M. Lieber, Nature (London) **375**, 769 (1995); W. Han, S. Fan, Q. Li, and Y. Hu, Science **277**, 1287 (1997).
²³Y. Zhang and H. Dai, Appl. Phys. Lett. **77**, 3015 (2000); Y.

- Zhang, N. W. Franklin, R. J. Chen, and H. Dai, *Chem. Phys. Lett.* **331**, 35 (2000).
- ²⁴S. Dag, E. Durgun, and S. Ciraci, *Phys. Rev. B* **69**, 121407(R) (2004).
- ²⁵C. K. Yang, J. Zhao, and J. P. Lu, *Phys. Rev. Lett.* **90**, 257203 (2003).
- ²⁶C. Zhou, J. Kong, and H. Dai, *Phys. Rev. Lett.* **84**, 5604 (2000).
- ²⁷F. Leonard and J. Tersoff, *Phys. Rev. Lett.* **84**, 4693 (2000); S. Dag, O. Gülseren, T. Yildirim, and S. Ciraci, *Appl. Phys. Lett.* **83**, 3180 (2003).
- ²⁸X. X. Zhang, G. H. Wen, S. Huang, L. Dai, R. Gao, and Z. L. Weng, *J. Magn. Magn. Mater.* **231**, L9 (2001); B. C. Satishkumar, A. Govindaraj, P. V. Vanitha, A. K. Raychaudhuri, and C. N. R. Rao, *Chem. Phys. Lett.* **362**, 301 (2002).
- ²⁹E. Durgun, S. Dag, V. K. Bagci, O. Gülseren, T. Yildirim, and S. Ciraci, *Phys. Rev. B* **67**, 201401(R) (2003); E. Durgun, S. Dag, S. Ciraci, and O. Gülseren, *J. Phys. Chem. B* **108**, 575 (2004).
- ³⁰M. R. Pederson and J. Q. Broughton, *Phys. Rev. Lett.* **69**, 2689 (1992).
- ³¹P. M. Ajayan and S. Iijima, *Nature (London)* **361**, 333 (1993).
- ³²Y. Gao, Y. Bando, Z. Liu, D. Goldberg, and H. Nakanishi, *Appl. Phys. Lett.* **83**, 2913 (2003).
- ³³Numerical computations have been carried out by using VASP software: G. Kresse and J. Hafner, *Phys. Rev. B* **47**, 558 (1993); G. Kresse and J. Furthmüller, *ibid.* **54**, 11169 (1996).
- ³⁴J. P. Perdew, J. A. Chevary, S. H. Vosko, K. A. Jackson, M. R. Pederson, D. J. Singh, and C. Fiolhais, *Phys. Rev. B* **46**, 6671 (1992).
- ³⁵H. J. Monkhorst and J. D. Pack, *Phys. Rev. B* **13**, 5188 (1976).
- ³⁶D. Sánchez-Portal, E. Artacho, J. Junquera, P. Ordejón, A. Garcia, and J. M. Soler, *Phys. Rev. Lett.* **83**, 3884 (1999).
- ³⁷H. Hakkinen, R. N. Barnett, and U. Landman, *J. Phys. Chem. B* **103**, 8814 (1999).
- ³⁸F. D. Tolla, A. D. Corsa, J. A. Torres, and E. Tosatti, *Surf. Sci.* **947**, 454 (2000).
- ³⁹P. Sen, S. Ciraci, A. Buldum, and I. P. Batra, *Phys. Rev. B* **64**, 195420 (2001).
- ⁴⁰S. Tongay, E. Durgun and S. Ciraci, *App. Phys. Lett.* (to be published).
- ⁴¹W. T. Geng and K. S. Kim, *Phys. Rev. B* **67**, 233403 (2003).
- ⁴²R. Landauer, *Z. Phys. B: Condens. Matter* **68**, 217 (1987).
- ⁴³S. Ciraci, T. Yildirim, S. Dag, O. Gülseren, and R. T. Senger, *J. Phys.: Condens. Matter* **16**, R901 (2004).
- ⁴⁴X. Blase, L. X. Benedict, E. L. Shirley, and S. G. Louie, *Phys. Rev. Lett.* **72**, 1878 (1994).
- ⁴⁵O. Gülseren, T. Yildirim, and S. Ciraci, *Phys. Rev. Lett.* **87**, 116802 (2001).
- ⁴⁶O. Gülseren, T. Yildirim, and S. Ciraci, *Phys. Rev. B* **65**, 153405 (2002).
- ⁴⁷B. L. Altshuler and A. G. Aronov, in *Electron-Electron Interaction in Disordered Systems*, edited by A. L. Efros and M. Polale (Elsevier, Amsterdam, 1985).
- ⁴⁸S. W. Ip, R. Sridhar, J. M. Toguri, T. F. Stephenson, and A. E. M. Warner, *Mater. Sci. Eng., A* **224**, 31 (1998).